Sea Target Classification Based on An A Priori Motion Model

Jimmy Bondu*†, Éric Grivel†, Audrey Giremus†, Pierrick Legrand‡, Vincent Corretja*, Marie Pommier*
*Thales Defence Mission Systems, Mérignac, FRANCE
†University of Bordeaux - INP Bordeaux ENSEIRB-MATMECA - IMS - UMR CNRS 5218, Talence, FRANCE
‡University of Bordeaux - IMB - UMR CNRS 5251 - Inria Bordeaux Sud-Ouest, Talence, FRANCE

***Abstract*—Target classification can be of real interest for sea surveillance in both civil and military contexts. To address this issue, we present two approaches based on the Singer model. The latter has the advantage of covering a wide range of motions depending on the values of its parameters. Given noisy observations, the first method aims at estimating the motion model parameters by taking advantage of the properties of the correlation function of the estimated acceleration. It is based on a genetic algorithm. The second approach is on-line and consists in deriving a joint tracking and classification (JTC) method. Based on various simulations, we study their respective relevance in different operational settings. The proposed JTC corresponds to the best compromise in terms of performance and number of samples required.**

***Index Terms*—Sea target classification, Singer model, Joint tracking and classification, Genetic algorithm, Correlation function**

I. Introduction

In the context of sea surveillance, ship classification is a widely studied topic. It finds applications in both civil and military activities, *e.g.* coastal port management, maritime risk analysis and prevention, illegal operation detection, maritime traffic pattern analysis [1]. The main source of data for vessel-type identification is the tracking information. The latter can be obtained with a GPS or a radar and/or the automatic identification system (AIS). These three systems send out the position of a vessel and update it frequently.

Several families of trajectory-based boat-type classification approaches have been proposed in the literature. The first family gathers the off-line algorithms and can be divided into two sub-families: those which process the whole trajectory, and conversely those in which the trajectory is decomposed into sub-trajectories. For the first sub-family, one can distinguish:

1) the algorithm suggested by Pelot and Wu in [2], where seven trajectory features, such as the mean velocity, the mean turning angle and the total distance travelled are extracted and correspond to the inputs of a classifier.

2) the method presented in [3], where down-sampled versions of the original trajectories are compared one another to determine similarities and then deduce clusters.

3) the deep-learning based approaches, which use various kinds of neural networks to address the classification issue [4], [5].

In the second sub-family, some authors suggest processing the sub-trajectories as segments without taking into account their intrinsic properties [6], [7]. Therefore, their methods do not manage to discriminate two kinds of ships if they have the same movement pattern. To overcome this limitation, other authors [8], [9] have proposed to first recognize movement patterns in the whole trajectory in order to split it into different sailing-phase sub-trajectories, such as anchored-off or straight-line. Then, specific features related to those sailing phases are extracted. These features are for instance the stop time, the main course and the small angle turn count. Furthermore, the performance of some previous methods can be improved by integrating geographical information, such as anchoring areas or harbor types [3].

The second big family, *i.e.* the on-line approaches, take their origins in the field of Bayesian target tracking. They are not specifically designed for classification but consist in improving trajectory estimation by jointly identifying the class of the targets which can be directly related to their degrees of maneuverability. The principle of joint tracking and classification (JTC) methods is to consider different *a priori* classes, each of them being associated to a set of motion models, and then to run a bank of filters based on the considered representations. The outputs of these filters make it possible to estimate the posterior probabilities of the different classes. In the end, they are combined to yield the final estimate of the target position and kinematics at each time step. If each class is associated to a single motion model, Kalman filters are classically considered. Conversely, if the values of the model parameters are unknown, multiple-model-based methods or Bayesian nonparametric models combined with particle filtering [10] can be implemented. However, the JTC becomes computationally intensive. It should be noted that additional information such as the target length extent measurement is often used to obtain more reliable results [11].

In this study, we propose and compare two model-based vessel-classification methods. In both, Singer models are considered, the parameters of which determine the boat category. The first one is a new off-line approach based on the properties of the estimated acceleration of the target. The second one is a voluntarily simplified JTC in which a single model per class with pre-defined parameters is considered. We also assume that only noisy position observations are available. This ensures a fair comparison between both techniques in terms of computational complexity and input information.

The rest of this paper is organized as follows: in section II the Singer model is recalled. Then, the method based on the properties of the correlation function of the estimated acceleration and the JTC approach are presented in section III. In section IV, the two methods are compared in terms of classification performance. Finally, conclusions and perspectives are drawn in section V.

II. Preamble: about Singer model

The Singer model is a motion model, for which the target acceleration $\ddot{x}_k$ is a time-correlated process. More particularly, the correlation function of the acceleration, $R_{\ddot{x}\ddot{x}}(\tau)$, exponentially decays with an exponential decay constant $\alpha > 0$:

$$R_{\ddot{x}\ddot{x}}(\tau) = \sigma_m^2 e^{-\alpha|\tau|T} = \sigma_m^2 \rho^{|\tau|} \quad (1)$$

where τ is the lag, T is the sampling rate, $\rho = e^{-\alpha T}$, and σ_m^2 is the variance of the target acceleration.

The Singer model has the advantage of covering other models such as the constant-acceleration (CA) motion model and the constant-velocity (CV) model when α tends to 0 and to infinity respectively.

It is often used as a state model for target tracking. In one dimension, when noisy position measurements are directly available, the corresponding state space representation is:

$$\begin{cases} \underline{x}_{k+1} = \Phi \underline{x}_k + G\underline{u}_k \\ y_k = H\underline{x}_k + n_k \end{cases} \quad (2)$$

where:

- $\underline{x}_k = \begin{bmatrix} x_k & \dot{x}_k & \ddot{x}_k \end{bmatrix}^t$ is the state vector at time k, with x_k the position, $\dot{x}_k$ the velocity at time k and t the transpose. Note that in two or three dimensions, the global state vector stores the position, velocity and acceleration along each axis.
- $H = \begin{bmatrix} 1 & 0 & 0 \end{bmatrix}$ is the observation vector while Φ denotes the transition matrix equal to:

$$\Phi = \begin{bmatrix} 1 & T & \frac{1}{\alpha^2}(\alpha T - 1 + \rho) \\ 0 & 1 & \frac{1}{\alpha}(1-\rho) \\ 0 & 0 & \rho \end{bmatrix} \quad (3)$$

- $G\underline{u}_k = G \begin{bmatrix} u_{1,k} & u_{2,k} & u_{3,k} \end{bmatrix}^t$ is the model noise with $\underline{u}_k$ a zero-mean Gaussian vector of covariance identity and G a lower triangular matrix, whose expression is a function of T, α and ρ that can be deduced from the covariance matrix Q of the model noise, given in [12].
- y_k is the noisy observation at time k, and n_k is a zero-mean additive white Gaussian noise with variance σ_n^2 which is uncorrelated with $\underline{u}_k$.

III. Two classification methods

A. Sea target classes

By specifying ranges of values of the Singer-model parameters, three sea target classes can be delineated. Thus, in Table I[1], the first class, whose name is *Cargo*, refers to the less maneuvering targets. The second one, called *Patrol boat*, includes the vessels which are more or less maneuvering, such as cabin cruisers, fishing boats or patrol boats. The last one, entitled *Fast boat*, refers to the most maneuvering targets, such as motorboats and jet skis. Fig. 1 gives examples of trajectories along one direction for each class.

[1]The orders of magnitudes have been provided by experts in the field.

TABLE I
Range of values of the Singer model parameters for the considered sea targets

Target class	α (s^{-1})	σ_m^2 $(m^2.s^{-4})$
c_1: *Cargo*	$\alpha \leq \alpha_{c_1,max} = 1/60$	$\sigma_m^2 \leq \sigma_{c_1,max}^2 = (0.02g)^2$
c_2: *Patrol boat*	$\alpha \leq \alpha_{c_2,max} = 1/40$	$\sigma_m^2 \leq \sigma_{c_2,max}^2 = (0.3g)^2$
c_3: *Fast boat*	$\alpha \leq \alpha_{c_3,max} = 1/5$	$\sigma_m^2 \leq \sigma_{c_3,max}^2 = (0.5g)^2$

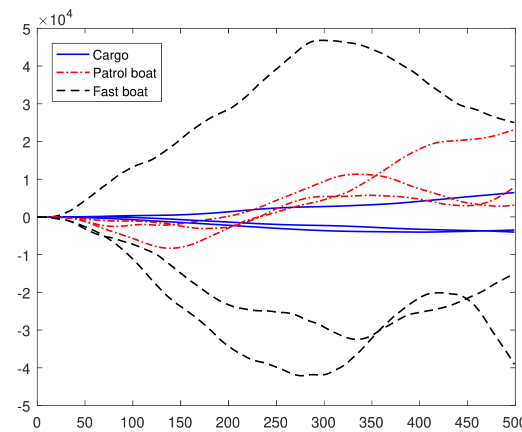

Fig. 1. Position x_k versus number of samples k. Examples for each class.

Given this *a priori* classification based on the motion model parameters, the two proposed methods are now presented.

B. Method based on the estimated acceleration properties

In this method, the parameters of the Singer model and the noise variance are estimated from the noisy observations. To this end, the theoretical correlation function of the estimated acceleration of the noisy observations is first deduced. Then, the model parameters are estimated so that the first terms of the unbiased estimation of the correlation function of the noisy-position acceleration match the theoretical ones.

In practice, the acceleration is not directly available from the recorded measurements. Therefore, when noise-free observations of the positions are available, it is common to estimate the acceleration with the following expression:

$$\hat{\ddot{x}}_k = \frac{x_k - 2x_{k-1} + x_{k-2}}{T^2} \quad (4)$$

Given (2)-(4), the estimated acceleration $\hat{\ddot{x}}_k$ can be expressed as a function of the theoretical acceleration as follows:

$$\hat{\ddot{x}}_k = A\ddot{x}_{k-1} + Bu_{1,k} + Cu_{1,k-1} + Du_{2,k-1} + Fu_{3,k-1} \quad (5)$$

where $A = \frac{4}{\alpha^2 T^2}\sinh^2\left(\frac{\alpha T}{2}\right)$, $B = \frac{G_{11}}{T^2}$, $C = \frac{G_{21}}{T} - \frac{G_{11}}{T^2} + \Delta G_{31}$, $D = \frac{G_{22}}{T} + \Delta G_{32}$, $F = \Delta G_{33}$ and $\Delta = -\frac{1}{\alpha^2 T^2}(e^{\alpha T} - \alpha T - 1)$, where G_{ij} is the element of G located at the i^{th} row and the j^{th} column.

Subsequently, if $\delta(\tau)$ denotes the Kronecker symbol, the correlation function of the estimated acceleration is given by:

$$\begin{aligned} R_{\hat{\ddot{x}}\hat{\ddot{x}}}(\tau) &= A^2 R_{\ddot{x}\ddot{x}}(\tau) + B\Big(AR_{\ddot{x}u_1}(\tau-1) + C\delta(\tau-1)\Big) \\ &+\Big(A(CG_{31}+DG_{32}+FG_{33}) + B^2 + C^2 + D^2 + F^2\Big)\delta(\tau) \\ &+A\Big(CR_{\ddot{x}u_1}(\tau) + DR_{\ddot{x}u_2}(\tau) + FR_{\ddot{x}u_3}(\tau)\Big) \end{aligned} \tag{6}$$

where:

$$R_{\ddot{x}u_i}(\tau) = G_{3i}\sum_{l=1}^{+\infty}\rho^{(l-1)}\delta(\tau+1-l) \tag{7}$$

Thus, one has:

$$\begin{aligned} R_{\hat{\ddot{x}}\hat{\ddot{x}}}(0) = A\Big(A\sigma_m^2 + 2(CG_{31}+DG_{32}+FG_{33})\Big) \\ + B^2 + C^2 + D^2 + F^2 \end{aligned} \tag{8}$$

$$\begin{aligned} R_{\hat{\ddot{x}}\hat{\ddot{x}}}(1) = \rho A\Big(A\sigma_m^2 + (CG_{31}+DG_{32}+FG_{33})\Big) \\ + B(AG_{31}+C) \end{aligned} \tag{9}$$

$$\begin{aligned} R_{\hat{\ddot{x}}\hat{\ddot{x}}}(2) = \rho^2 A\Big(A\sigma_m^2 + (CG_{31}+DG_{32}+FG_{33})\Big) \\ + AB\rho G_{31} \end{aligned} \tag{10}$$

$$\forall\ \tau \geq 3,\ \rho = \frac{R_{\hat{\ddot{x}}\hat{\ddot{x}}}(\tau)}{R_{\hat{\ddot{x}}\hat{\ddot{x}}}(\tau-1)} \underset{(1)}{=} \frac{R_{\ddot{x}\ddot{x}}(\tau)}{R_{\ddot{x}\ddot{x}}(\tau-1)} \tag{11}$$

Given (8)-(10), for $\tau = 0, ..., 2$, $R_{\hat{\ddot{x}}\hat{\ddot{x}}}(\tau)$ is equal to $R_{\ddot{x}\ddot{x}}(\tau)$, up to the multiplicative constant A^2 and an additive term depending on α and T. When noisy observations are available, by combining (2) and (4), the estimated acceleration $\hat{\ddot{y}}_k$ of the noisy observations satisfies:

$$\hat{\ddot{y}}_k = \frac{y_k - 2y_{k-1} + y_{k-2}}{T^2} = \hat{\ddot{x}}_k + \hat{\ddot{n}}_k \tag{12}$$

where $\hat{\ddot{n}}_k = \frac{n_k - 2n_{k-1} + n_{k-2}}{T^2}$. The correlation function of the estimated acceleration of the noisy observations hence satisfies:

$$R_{\hat{\ddot{y}}\hat{\ddot{y}}}(\tau) = R_{\hat{\ddot{x}}\hat{\ddot{x}}}(\tau) + R_{\hat{\ddot{n}}\hat{\ddot{n}}}(\tau) \tag{13}$$

where:

$$R_{\hat{\ddot{n}}\hat{\ddot{n}}}(\tau) = \frac{\sigma_n^2}{T^4}(6\delta(\tau) - 4(\delta(\tau-1)+\delta(\tau+1)) + \delta(\tau-2) + \delta(\tau+2)) \tag{14}$$

So, the correlation functions $R_{\hat{\ddot{x}}\hat{\ddot{x}}}(\tau)$ and $R_{\hat{\ddot{y}}\hat{\ddot{y}}}(\tau)$ are the same in theory for $\tau \geq 3$. Therefore, using (11), one has $\forall\ \tau \geq 4$:

$$\rho = \frac{R_{\ddot{x}\ddot{x}}(\tau)}{R_{\ddot{x}\ddot{x}}(\tau-1)} = \frac{R_{\hat{\ddot{x}}\hat{\ddot{x}}}(\tau)}{R_{\hat{\ddot{x}}\hat{\ddot{x}}}(\tau-1)} = \frac{R_{\hat{\ddot{y}}\hat{\ddot{y}}}(\tau)}{R_{\hat{\ddot{y}}\hat{\ddot{y}}}(\tau-1)} \tag{15}$$

The above relation seems *a priori* appealing, but, in practice, the unbiased estimation of the acceleration of the noisy positions, denoted as $\hat{R}_{\hat{\ddot{y}}\hat{\ddot{y}}}(\tau)$, is used and can lead to a poor estimate of ρ for $\tau \geq 3$. This mainly depends on the values taken by the model parameters and the number of samples. For this reason, we propose to jointly estimate all the model parameters by minimising the following criterion:

$$J(\alpha, \sigma_m^2, \sigma_n^2) = \sum_{\tau=0}^{2}(R_{\hat{\ddot{y}}\hat{\ddot{y}}}(\tau; \alpha, \sigma_m^2, \sigma_n^2) - \hat{R}_{\hat{\ddot{y}}\hat{\ddot{y}}}(\tau))^2 \tag{16}$$

where $R_{\hat{\ddot{y}}\hat{\ddot{y}}}(\tau; \alpha, \sigma_m^2, \sigma_n^2)$ is the theoretical correlation function of the estimated acceleration of the noisy observations evaluated for α, σ_m^2 and σ_n^2 by combining (8)-(10) and (13). Searching for the solution of this optimization issue is not straightforward. Indeed, it is difficult to derive a closed-form expression of the elements of the matrix G appearing in the correlation function $R_{\hat{\ddot{y}}\hat{\ddot{y}}}(\tau; \alpha, \sigma_m^2, \sigma_n^2)$. This makes the gradient computation of (16) intricate. Therefore, we suggest using a genetic algorithm (GA) [13]. Its purpose is to optimize a function, called fitness, until a stop criterion is reached. To this end, a population of potential solutions improves its characteristics over iterations, through a series of basic genetic operations called selection, mutation and genetic recombination or crossing. To operate, the GA works as follows:

1) Given the noisy observations available, the correlation function of the estimated acceleration is estimated.
2) Let N be the size of the population. All population individuals, which are vectors $\theta^{(i)} = [\alpha^{(i)}, \sigma_m^{2(i)}, \sigma_n^{2(i)}]$, with $i = 1, ..., N$, are randomly set. For each individual, as T is *a priori* known, Δ and Q can be defined. Hence, G or equivalently its elements $\{G_{ij}\}$ can be deduced. Therefore, A, B, C D and F can be obtained. $R_{\hat{\ddot{y}}\hat{\ddot{y}}}(\tau; \alpha, \sigma_m^2, \sigma_n^2)$ and consequently the fitness function, which is (16) in our case, can be evaluated.
3) Selections are performed in the form of a tournament: two individuals are randomly selected and the one with the best fitness score is kept. Each time, this process is repeated twice to obtain two parents, denoted as $\theta^{(p_1)}$ and $\theta^{(p_2)}$. The latter are used to generate a new individual by using a barycentric combination. Given $0 < \varepsilon < 1$, this leads to: $\theta^{(c)} = \varepsilon\theta^{(p_1)} + (1-\varepsilon)\theta^{(p_2)}$. The new obtained individual is subject to a mutation, *i.e.* a random modification of its parameters, with the probability p_m. This mutation consists in adding a zero-mean Gaussian noise with a suited variance. This can prevent the GA to be stuck in a local minimum.
4) The new individuals are evaluated with (16) before being replaced into the initial population.
5) The best individuals are kept and a new iteration is proceeded until a number of iterations is reached.

The best individual of the last population corresponds to the estimation of the model parameters, namely $\hat{\alpha}$, $\hat{\sigma}_m^2$ and $\hat{\sigma}_n^2$. Among the possible decision rules, the following one is considered in this paper:

$$\hat{c} = \underset{\{c_i\}_{i=1,...,3}}{\arg\min}\left\{\frac{(\hat{\alpha} - \alpha_{c_i,max})^2}{\alpha_{c_i,max}^2} + \frac{\left(\hat{\sigma}_m^2 - \sigma_{c_i,max}^2\right)^2}{\left(\sigma_{c_i,max}^2\right)^2}\right\} \tag{17}$$

with $\{\alpha_{c_i,max}\}_{i=1,...,3}$ and $\{\sigma_{c_i,max}^2\}_{i=1,...,3}$ given in Table I. In the presence of nested classes, it tends to favor the encompassing one.

C. JTC technique

JTC approaches are a category of Bayesian dynamic inference methods originally dedicated to target tracking. As such, they estimate the time-varying kinematic parameters of a target by using not only the information from the sensors but also prior probabilistic evolution models. JTC techniques take advantage of the fact that, depending on their characteristics (length, etc.), the targets exhibit different degrees of maneuverability. They consist in identifying the target type while estimating its trajectory and dynamics, both issues being closely related. In the first place, classes of targets are pre-defined and they are associated with collections of representative motion models. Then, the target of interest is assigned a label indicating its class, which is estimated along with the state vector in the Bayesian sense. For that purpose, a bank of tracking algorithms is run: each of them is based on a class hypothesis and therefore uses a specific set of state models.

Different JTC variants exist depending on the estimation algorithms. They can be multiple-model filters, or merely Kalman filters (KFs) if two conditions are met: a single model per class is considered and it is linear Gaussian as well as the observation model. It is the case in our framework wherein we propose to rely on the state space representation (2). A class is then merely identified by a given value of the parameters α and σ_m^2 of the Singer state model.

If $c \in \{c_1, \dots, c_3\}$ denotes the target class, the KF associated to the class c computes at iteration k the conditional posterior distribution of the state vector $p(x_k|y_{1:k}, c)$, which is Gaussian[2]. The conditional distribution of the current observation $p(y_k|y_{1:k-1}, c)$ comes as a by-product. It is also Gaussian and serves for the class identification. If $\hat{x}^c_{k|k-1}$ and $P^c_{k|k-1}$ respectively stand for the state prediction and the covariance error matrix of the c^{th}-class KF, then this probability density function is expressed as:

$$p(y_k|y_{1:k-1}, c) \propto \exp\left[-\frac{(y_k - H\hat{x}^c_{k|k-1})^2}{2\left(HP^c_{k|k-1}H^t + \sigma_n^2\right)}\right] \tag{18}$$

where σ_n^2 is assumed to be known[3]. The decision in favor of a class is based on its posterior probability, which can be expressed recursively as follows:

$$\mathrm{P}\left[c|y_{1:k}\right] \propto p(y_k|y_{1:k-1}, c)\mathrm{P}\left[c|y_{1:k-1}\right] \tag{19}$$

where the proportionality coefficient is adjusted so that the sum of the probabilities over all the possible class labels equals 1.

Finally, it should be noted that the overall posterior distribution of the state, regardless of its class, can be estimated as a mixture of Gaussian probability density functions:

$$p\left(x_k|y_{1:k}\right) = \sum_{i=1}^{3} p(x_k|y_{1:k}, c_i)\mathrm{P}\left[c_i|y_{1:k}\right] \tag{20}$$

However, since we only use the JTC for classification purposes in this work, we do not apply this step of the algorithm. In this way, the computational complexity of the JTC is reduced.

[2]For the sake of space, the corresponding equations are not given but they are usually well-known and can be found in different books such as [14].

[3]This is a limitation of this approach.

IV. Experiments

A. Simulation protocol and classification strategy

To compare the performance of the two boat-type identification methods, 100 trajectories of K samples were generated for each class. Both parameters of the Singer models were drawn according to normal distributions, where the means were equal to the upper bounds of the intervals given in Table I and the variances were set to obtain overlaps between the classes. In addition, only the left sides of the tails were kept to represent the fact that fast or patrol boats are not necessarily maneuvering. Moreover, to simulate the measurement noise, a zero-mean Gaussian noise with a standard deviation $\sigma_n = 10\ m$ was added to each trajectory.

Concerning the JTC approach, the parameters of the three Singer models involved in this method were also set at the upper bounds of the intervals written in Table I. Note that it requires σ_n^2 to be known, but different techniques in the literature address this issue. Furthermore, we observed that the JTC is very robust to misadjustments of this parameter.

As for the GA algorithm, the hyperparameters are given by: $N = 500$, $\varepsilon = 0.5$ and $p_m = 0.2$. In addition, 200 iterations are done and the number of new individuals to create per iteration is set at 200.

B. Simulation results

To provide a fair comparison, the classification results are presented in the form of confusion matrices given in Table II and Table IV for the off-line and the on-line methods respectively. Moreover, for the off-line method, information about the accuracy of the parameter estimations is also provided.

TABLE II
Confusion matrices for the off-line approach ($K = 2000$)

(a) $T = 1$s

True labels (%) \ Predicted labels (%)	Cargo	Patrol boat	Fast boat
Cargo	15	61	24
Patrol boat	17	32	51
Fast boat	16	6	78

(b) $T = 10$s

True labels (%) \ Predicted labels (%)	Cargo	Patrol boat	Fast boat
Cargo	92	6	2
Patrol boat	11	89	0
Fast boat	4	13	83

As shown in Table II, the classification performance differs when $T = 1$s and $T = 10$s. This can be explained by the fact that the orders of magnitudes of the ratios $\{R_{\hat{x}\hat{x}}(\tau)/R_{\hat{n}\hat{n}}(\tau)\}_{\tau=0,\dots,2}$ are not the same. Indeed, when $T = 10$s, they are 10^3 to 10^4 times larger than the ones computed for $T = 1$s. As a consequence, the model parameters are better estimated, as shown by Fig. 2 (where the median relative error of an estimated parameter is represented by the square and its first and third quartile are respectively delineated by the lower and the upper bar).

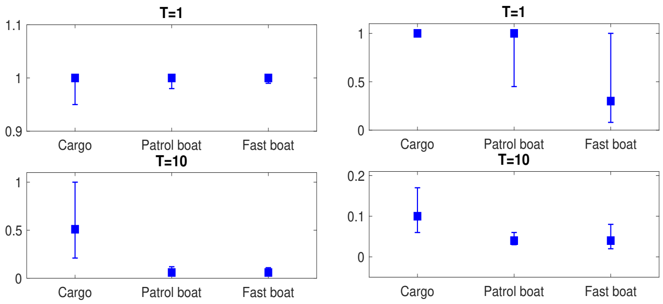

(a) α **(b)** σ_m^2

Fig. 2. Estimation relative error on both parameters for the off-line approach ($K = 2000$)

Let us now investigate the influence of the number of samples in the trajectory for $T = 10$s. As shown in the two illustrations gathered in Table III, the classification and the estimation performance are slightly lower than the ones exhibited in Table IIb and Fig. 2.

TABLE III
CONFUSION MATRIX (LEFT) AND ESTIMATION RELATIVE ERROR (RIGHT) FOR THE OFF-LINE APPROACH ($T = 10$S AND $K = 200$)

True labels (%) \ Predicted labels (%)	Cargo	Patrol boat	Fast boat
Cargo	83	14	3
Patrol boat	12	84	4
Fast boat	6	14	80

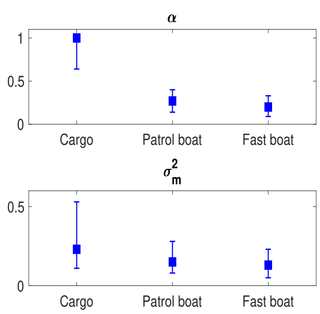

TABLE IV
CONFUSION MATRICES FOR THE JTC APPROACH WITH σ_n^2 *a priori* KNOWN ($K = 2000$)

(a) $T = 1$s

True labels (%) \ Predicted labels (%)	Cargo	Patrol boat	Fast boat
Cargo	100	0	0
Patrol boat	6	94	0
Fast boat	0	27	73

(b) $T = 10$s

True labels (%) \ Predicted labels (%)	Cargo	Patrol boat	Fast boat
Cargo	100	0	0
Patrol boat	5	95	0
Fast boat	0	26	74

Now, the performance of the proposed JTC is studied. As shown in Table IV, when the JTC is used, most of the generated trajectories are well-classified if the variance of the measurement noise is known. In addition, according to Fig. 3, the convergence is fast. Therefore, all the samples in the trajectories are not required and their number could be reduced as long as the performance remains satisfactory. It should be also noted that the classification errors are only made on the targets which are able to mimic the behavior of a less maneuvering target. Last but not least, note that in theory σ_n^2 is supposed to be *a priori* known. However, we observed in all the simulations we did that the approach remains robust to small misadjustments of its value.

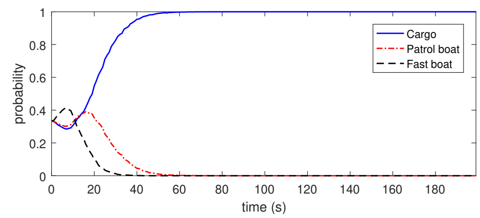

Fig. 3. Target class probabilities averaged over 100 Cargo trajectories ($T = 1$s)

V. CONCLUSION AND PERSPECTIVES

In this paper the target classification is addressed by considering an off-line approach and a JTC-based method, both based on the Singer model. Even if the off-line approach has the advantage of estimating the measurement noise variance, it is shown that the JTC algorithm outperforms it in terms of classification performance and number of samples required. As a perspective, we plan to investigate deep learning approaches.

REFERENCES

[1] M. Vespe, I. Visentini, K. Bryan, and P. Braca, "Unsupervised learning of maritime traffic patterns for anomaly detection," *Proceedings of 9th IET Data Fusion and Target Tracking Conference : Algorithms and Applications*, 2012.

[2] R. Pelot and Y. Wu, "Classification of recreational boat types based on trajectory patterns," *Pattern Recognition Letters*, vol. 28, no. 15, pp. 1987–1994, 2007.

[3] G. De Vries and M. Van Someren, "Machine learning for vessel trajectories using compression, alignments and domain knowledge," *Exp. Systems with Applications*, vol. 39, no. 18, pp. 13 426–13 439, 2012.

[4] H. Ljunggren, "Using deep learning for classifying ship trajectories," *Proceedings of Fusion*, pp. 2158–2164, 2018.

[5] R. Zhang, P. Xie, C. Wang, G. Liu, and S. Wan, "Classifying transportation mode and speed from trajectory data via deep multi-scale learning," *Computer Networks*, vol. 162, pp. 106 861–106 874, 2019.

[6] J.-G. Lee, J. Han, X. Li, and H. Gonzalez, "Traclass: trajectory classification using hierarchical region-based and trajectory-based clustering," *Proceedings of the VLDB Endowment*, pp. 1081–1094, 2008.

[7] M. Elwakdy, M. El-Bendary, and M. Eltokhy, "A novel trajectories classification approach for different types of ships using a polynomial function and anfis," *Proceedings of IPCV*, pp. 387–395, 2015.

[8] K. Sheng, Z. Liu, D. Zhou, A. He, and C. Feng, "Research on ship classification based on trajectory features," *The Journal of Navigation*, vol. 71, no. 1, pp. 100–116, 2018.

[9] P. Kraus, C. Mohrdieck, and F. Schwenker, "Ship classification based on trajectory data with machine-learning methods," *Proceedings of IRS*, pp. 1–10, 2018.

[10] C. Magnant, A. Giremus, E. Grivel, L. Ratton, and B. Joseph, "Bayesian non-parametric methods for dynamic state-noise covariance matrix estimation: Application to target tracking," *Signal Processing*, vol. 127, pp. 135–150, 2016.

[11] L. Legrand, A. Giremus, E. Grivel, L. Ratton, and B. Joseph, "Bernoulli filter based algorithm for joint target tracking and classification in a cluttered environment," *Proceedings of ICASSP*, pp. 4396–4400, 2017.

[12] R. A. Singer, "Estimating optimal tracking filter performance for manned maneuvering targets," *IEEE Transactions on Aerospace and Electronic Systems*, no. 4, pp. 473–483, 1970.

[13] J. H. Holland, *Adaptation in natural and artificial systems: an introductory analysis with applications to biology, control, and artificial intelligence*. University of Michigan press Ann Arbor, 1975.

[14] Y. Bar-Shalom, P. Willett, and X. Tian, *Tracking and data fusion: a handbook of algorithms*. YBS Publishing, 2011.